Global regulatory factor FsveA up-regulate the production of antitumor substance in endophytic *Fusarium solani*

Lu Cai
Jiankang Wang
Yongjie Li
Min Qin
Xueming Yin
Zhangjiang He (zjhe3@gzu.edu.cn)
Guizhou University of Technology: Guizhou University https://orcid.org/0000-0002-7120-1227
Jichuan Kang

Research Article

Keywords: Endophytic Fusarium solani, Global regulatory factor FsveA, Antitumor activity, Metabolomics, Transcriptomics

Posted Date: March 10th, 2022

DOI: https://doi.org/10.21203/rs.3.rs-1414066/v1

Abstract

A number of studies have demonstrated that endophytic fungi have the potential to produce antitumor active substances with novel structures and significant activities. Our previous studies found that an endophytic *Fusarium solani* derived from the stem of the medicinal plant *Nothapodytes pittosporoides* (Oliv.) Sleum had good antitumor activity. Furthermore, overexpression of the global regulator *FsveA* (*FsveA*^{OE}) in *F. solani* led to significant inhibition ratio increasement of human alveolar adenocarcino -ma cell (A549). In comparison with the wild strain (WT), the inhibition rate of FsveA^{OE} was obviously increased ~ 14.69%, and the apoptosis ratio was significantly increased 4.86-fold. A metabolomic analysis revealed that the overexpression of *FsveA* resulted in a significant increasement in several antitumor secondary metabolites of fungi, including alkaloids (Geldanamycin, Acadesine, Adenosine), terpenoids (Lanosterin, Illudin M), carboxylic acid derivatives (L-Arginine, L-Methionine), phenolic (4-Allyl-2-methoxyphenol) and flavonoid metabolites (Epicatechin gallate). Additionally, the transcriptome analysis also displayed that expression pattern of 48 genes-related to the antitumor activity were significantly changed in *FsveA*^{OE}, mainly involving glycosyl hydrolases, the Zn(2)-Cys(6) class, Cytochrome P450 monooxygen -ase, 3-isopropylmalate dehydratase, and polyketide synthases. Therefore, we conclude that *FsveA* mediate multiple secondary metabolic pathways to up-regulate the production of antitumor substance in endophytic *F. solani.*

Introduction

Cancer is a common and frequently-occurring disease threatening human health. According to a report from the World Health Organization (WHO), cancer-related deaths will increase and are expected to reach an approximate number of 11.5 million by 2030 all over the world (Ur Rashid et al. 2020). As an important means of cancer treatment, Drug therapy has been the fastest in growth (Shan et al. 2005). However, the existing anticancer drugs are confronted with toxic side effects and drug resistance. While coexisting with their host plant in the nature, endophytic fungi have a special symbiotic relationship with the hosts (Terkar and Borde, 2021; Li et al. 2018). A number of studies have demonstrated that endophytic fungi have the potential to produce antitumor active substances with novel structures and significant activities. (Chen et al. 2016; Teixeira et al. 2019; Bedir et al. 2021; He et al. 2020). Moreover, endophytic *Fusarium solani* produced secondary metabolites with the potential for antitumor activity, including camptothecin with inhibitory activity on cancer cells (Ran et al. 2017) and Azaanthra -quinone derivatives with cytotoxic activity against four human tumor cell lines, MDAMB231, MIAPaCa2, HeLa, and NCIH1975 (Chowdhury et al. 2017). Therefore, it is important to carry out studies on the antitumor activity of endophytic *F. solani*.

With the deepening studies on endophytic fungi, researchers have found that most biosynthetic gene clusters in filamentous fungi are silenced under conventional laboratory culture conditions, and these silenced gene clusters contain an abundant resource of secondary metabolites (Wei et al. 2021). In recent years, the use of regulatory factor strategies to activate silenced genes in strains to screen for new structures and high-activity secondary metabolites is becoming a research hotspot (Lyu et al. 2020). The global regulatory factor *veA* is a velvet-like photosensitive protein firstly identified in *Aspergillus nidulans*

whose N-terminal contains a highly conserved nuclear localization region among different species, and the C-terminal contains a PEST region (Ma et al. 2012). In fungi, it is found that the gene can positively regulate sexual reproduction and negatively regulate asexual reproduction, and it is a necessary gene for the biosynthesis of some fungal metabolites, which has a great influence on mycelial morphology and metabolites (Kim et al. 2009). Studies have shown that *veA* negatively regulates penicillin biosynthesis in *Penicillium chrysogenum* (Kopke et al. 2013). *veA* in *Pestalotiopsis microspora* is different from most *veA* in inhibiting asexual reproduction and activating the synthesis of secondary metabolites, it positively regulates the production of conidia and mycelial growth but negatively regulates the synthesis of pestalotiollide B (Akhberdi et al. 2018). This indicated that *veA* in different strains had special effects on metabolism and morphological differentiation, which provided a new way for the development of natural products in fungi.

At present, there were few reports on whether *veA* mediates the anti-tumor activity of endophytic fungi. Our previous studies have found an endophytic *Fusarium solani* HB1-J1 derived from the plant *Nothapodytes pittosporoides* (Oliv.) Sleum with good and stable antitumor activity. In order to further study the anti-tumor activity of this strain, we over-expressed the fungal conservative global regulatory factor *FsveA* in this strain. Transcriptome and metabolomics analyses were performed to explore the effect of *veA* on the antitumor activity, as well as regulation of secondary metabolism and growth and development of *F. solani*.

Materials And Methods

Identification of Endophytic *Fusarium solani* HB1-J1

Seeded into PDA plates, the isolated and purified strain HB1-J1 was cultured for 7 days (d) at 28 ℃. Observe the colony morphology and color, and measure the diameter. To observe the morphological characteristics of conidia, conidiogenous cells, and chlamydospore under the microscopic field of view for preliminary identification (Qiu et al. 2020). Images were processed using Adobe Photoshop CS6 software.

Genomic DNA was extracted from the strain using a fungal genomic DNA extraction kit (Biomiga). Amplification was performed using primers ITS1/ITS4 (White et al. 1990), EF-1/EF-2 (Geise et al. 2004), RPB1-DF2asc/RPB1-G2R (Zhang et al. 2020), fRPB2-5f2/fRPB2-7cr (Qiu et al. 2020). Sequencing was done on the PCR products. After performing the nucleotide BLAST of sequencing product, the fasta sequence of similar organisms along with nearest neighbor sequences from the NCBI database were download (Table S1) and comparison by online server MAFFT v.7.110 (Katoh and Standley, 2013; Soni et al. 2021; Ameen et al. 2021). The spliced dataset (Vaidya et al. 2011) was analyzed phylogenetically using the online software CIPRES Science Gateway v.3.3 (Assunção et al. 2020). Phylogenetic trees were edited by FigTree v1.4.4.

Construction of a genetic transformation system in *Fusarium solani*

The target fragments were obtained by PCR amplification with specific primers *veA*-F/*veA*-R, *PgpdA*-Xba1-F /*PgpdA*-*veA*-R (Table S2) using DNA from the strain and *PgpdA* plasmid as templates. *PgpdA*::*veA* fusion product and pK_2hyg backbone vector were double enzyme digested with *Xba* 1 and *Hin*d III, and T_4DNA ligated before being transferred into *E.coli* DH5α competent cells by the thermal stimulation method. After verifying the correct vector by colony amplification, enzyme digestion, and sequencing, the pK_2*hyg*-PgpdA-veA plasmid was transformed into *Agrobacterium tumefaciens* by electroshock method. Then it was transferred into the HB1-J1 strain by *Agrobacterium*-mediated (Ma et al. 2009).

FsveA gene sequence analysis

The *FsveA* gene was analyzed by an online BLAST search at the NCBI Web site. For the multiple sequence alignment analysis, the amino acid sequences of *FsveA* and other *veA* homologues from different species retrieved from NCBI were aligned using the online server MAFFT v.7.110 (Katoh and Standley, 2013). The phylogenetic analysis was conducted with the MEGA7 software. GENEDOC was used to treat the *FsveA* protein's conserved domain.

Real-time Quantitative PCR analysis

Mycelia of WT and *FsveA*^{OE} fermented in Sabouraud's liquid medium for 7 d were collected, and total RNA was extracted by the Easy Spin Plant RNA Rapid Extraction Kit from Adelaide. Total RNA quality and concentration were detected, and DNA was removed after extraction was completed. cDNA was synthesized by referring to the GenStar kit, and cDNA was used as a template for RT-qPCR analysis. Using the *tubulin* gene in *Fusarium* as an internal reference gene (Alexander et al. 2018). Relative expression levels of each gene was calculated by the comparative crossing point method and presented as $2^{-\Delta\Delta Ct}$. Each gene expression analysis was performed with three independent biological replicates. The specific primers used for RT-qPCR are listed in Table S2.

Preparation of crude extracts

The blastospore of *FsveA*^{OE} and wild-type HB1-J1 strains were quantitatively inoculated into Sabouraud's liquid medium and fermented aerobically at 28 ℃ and 180 rpm for 7 d. Fermentation cultures of mutant and WT strains were extracted three times with ethyl acetate and concentrated under decreased pressure to obtain crude extracts for anti-tumour activity and metabolomics assays (filter mycelia stored at -80 ℃for transcriptome detection). Metabolome and transcriptome detection were entrusted to Biomarker Technologies (https://international.biocloud.net/zh/user/login).

Proliferation of cancer cells by MTT assay

Human alveolar adenocarcinoma cells (A549) in the logarithmic growth phase and in good growth conditions were taken and digested with trypsin, and the addition of RPMI1640 fresh medium containing serum terminated the reaction. Centrifugation to make cell suspension, inoculation in 96-well plates at 1×10^6 cells/mL, 100 μL per well, incubation at 37 ℃, 5 % CO_2 incubator for 24 hours (h). Different drug

concentrations were prepared with fresh medium, and five duplicate wells were set for each concentration. The crude extract was utilized as the experimental group, the adriamycin was used as the positive control, the medium containing only cells was used as the negative control, and the culture time was 48 h. Then 20 μL of MTT solvent was added to each well, incubated for 4 h, the supernatant was discarded, and DMSO 150 μL/well was added. At 490 nm, the absorbance was measured using an enzyme-labeled device.

Detection of apoptosis by AnnexinV-FITC/PI

A549 cells at the logarithmic growth stage were taken, made into cell suspension, inoculated into 6-well plates at 1×10^7 cell/mL, 1 ml per well, and incubated in a 5 % CO_2 incubator at 37 ℃for 24 h. Then, WT and *FsveA*^{OEV14} crude extracts were applied to the cells for 48 h. The cells were collected, washed in 1xPBS, centrifuged, stained with AnnexinV-FITC/PI reagent kit, and flow cytometry was than used to detect apoptosis of the cells.

Nontarget LC-MS/MS metabolome detection

Waters Xevo G2-XS QTOF high resolution mass spectrometer was used to collect primary and secondary mass spectrometry data in MSe mode under the control of the acquisition software (MassLynx V4.2,Waters). In each data acquisition cycle, dual-channel data acquisition can be performed on both low collision energy and high collision energy at the same time. The low collision energy is 2 V, the high collision energy range is 10~40 V, and the scanning frequency is 0.2 seconds for a mass spectrum. The parameters of the ESI ion source are as follows: Capillary voltage: 2000 V (positive ion mode) or -1500 V (negative ion mode); cone voltage: 30 V; ion source temperature: 150 ℃; desolvent gas temperature 500 ℃; backflush gas flow rate: 50 L/ hours; Desolventizing gas flow rate: 800 L/hours.

Transcriptome sequencing

The purity, concentration and integrity of RNA samples were tested using advanced molecular biology equipment to ensure the use of qualified samples for transcriptome sequencing. A total amount of 1μg RNA per sample was used as input material for the RNA sample preparations. Sequencing libraries were generated using NEBNext®Ultra™RNALibrary Prep Kit for Illumina®(NEB, USA) following manufacturer's instructions and index codes were added to attribute sequences of each sample. Briefly, mRNA was purified from total RNA using poly-T oligo-attached magnetic beads. Fragmentation was carried out using divalent cations under elevated temperature in NEBNext First Strand Synthesis Reaction Buffer（5X）. First strand cDNA was synthesized using random hexamer primer and M-MuLV Reverse Transcriptase. Second strand cDNA synthesis was subsequently performed using DNA Polymerase I and RNase H. Remaining overhangs were converted into blunt ends via exonuclease/polymerase activities. After adenylation of 3, ends of DNA fragments, NEBNext Adaptor with hairpin loop structure were ligated to prepare for hybridization. In order to select cDNA fragments of preferentially 240 bp in length, the library fragments were purified with AMPure XP system (Beckman Coulter, Beverly, USA). Then 3μL USER Enzyme (NEB, USA) was used with size-selected, adaptor-ligated cDNA at 37 ℃ for 15 min followed by 5 min at

95 ℃ before PCR. Then PCR was performed with Phusion High-Fidelity DNA polymerase, Universal PCR primers and Index (X) Primer. At last, PCR products were purified (AMPure XP system) and library quality was assessed on the Agilent Bioanalyzer 2100 system. The clustering of the index-coded samples was performed on a cBot Cluster Generation System using TruSeq PE Cluster Kit v3-cBot-HS (Illumia) according to the manufacturer's instructions. After cluster generation, the library preparations were sequenced on an Illumina Hiseq 2000 platform and paired-end reads were generated.

Statistical analysis

One-way ANOVA was used to examine the findings of the qRT-PCR studies, and $P < 0.05$ was considered statistically significant. The results of anti-tumor activity data and apoptosis data of each sample were analyzed using t-tests (and nonparametric tests), and the IC_{50} values were statistically analyzed using SPSS 12.0 software, all expressed in s(standard deviation). In metabolome and transcriptome analysis, Fold change (FC)> 1, variable projection significance assessment (VIP)> 1, and $P < 0.05$ thresholds were considered statistically significant.

Results

The crude extracts of endophytic *Fusarium solani* have anti-tumor activity

To investigate the antitumor activity of the endophytic strain HB1-J1, we examined the status of A549 test cell line using the MTT method with adriamycin as a positive drug. The survival rate of A549 decreased significantly with increasing concentration of adriamycin, and the IC_{50} was 3.84±1.67 μg/ml (Fig. 1A), and the applied concentrati -on range was consistent with the literature (Xu et al. 2018; Xie et al. 2015; Zhu et al. 2012) , indicating that the A549 cell line was in normal status and could be used for the test. Compared with the negative control group, the ethyl acetate extract of HB1-J1 showed a significant inhibitory effect on A549 (P <0.05), which was increased with the increasement of the concentration of the crude extract. At a concentration of 300 μg/mL, the inhibition rate was 37.87 %, and the IC_{50} value was 362.21±1.34 μg/ml (Fig. 1B). The inhibitory effect on A549 of HB1-J1 was revealed.

In order to explore the antitumor substances of the strain, we firstly identified the fungus. Morphological observations revealed that the aerial mycelium of the strain on PDA medium was white villous, with neat colony edges and yellowish pigmentation on the back of the substrate (Fig. 2A). Conidiogenous structures were multi-typed (Fig. 2B,C, D). Conidia were of two types: microconidia, ellipsoidal, reniform, 44.9-62.5 μm; Macroconidia, falcate, beaked at both ends, 301.20-359.70 μm, 4-6 septate (Fig. 2G). Chlamydospore, spherical or ellipsoid, beaded chains, 3.00-8.86 μm in diameter (Fig. 2E-F). All the morphological structures were similar to those of *Fusarium* sp.. Meanwhile, ITS, EF1α, RPB1 and RPB2 multigene tandem sequences were used to construct phylogenetic tree with the outgroup *Fusarium oxysporum* LEMM110787 and find the closely related species of the fungus. The results showed that

strain HB1-J1 clustered with *Fusarium solani* on the same branch with 99% similarity (Fig. 2H). Therefore, the strain was identified as *F. solani*.

Overexpression of *FsveA* enhances the antitumor activity of the strain

To explore the effect of *FsveA* on the antitumor activity of the strain, the *FsveA* gene was overexpressed in the *F. solani* strain. The homologous gene of *veA* in this strain was amplified and sequenced using the *F. solani* genome as a template. Protein homology analysis revealed that the homologous protein was 86% homologous to *veA* of *F. solani* KAH7250457. Therefore, the protein was named *FsveA* (Fig. 3A, Fig. S1). Construction of the *veA* overexpression vector by replacing the promoter of the *FsveA* gene in WT with the constitutive promoter *PgpdA* of *Aspergillus nidulans* (Fig. 3B). *Via* Agrobacterium-mediated genetic transformation, wild-type and transformant strains were inoculated on CZM plates containing hygromycin B resistance, and WT growth was found to be significantly inhibited, while the transformants grew normally (Fig. 3C). Further PCR verification of the transformants by the hygromycin B resistance gene (hyg) carried by the pK_2*hyg*-PgpdA-veA vector showed that the transformants could be amplified with specific bands at about 1000 bp, which was consistent with the expected size, while WT had no band (Fig. 3D), demonstrating the overexpression mutant *FsveA*^{OE} was successful. The *FsveA* gene transcript levels of WT and transformants were also analyzed by qRT-PCR, and it was found that *FsveA*^{OEV14}, *FsveA*^{OEV12}, and *FsveA*^{OEV2} strains were significantly up-regulated 52.5, 12.1, and 10.35 fold (P<0.005) compared to WT (Fig. 3E). MTT method was used to detect the anti-tumor activity of the crude extracts of *FsveA*^{OEV14}, *FsveA*^{OEV12}, *FsveA*^{OEV2}, and WT strains. Results showed that the difference in activity of crude extracts between WT and *FsveA*^{OEV14} was significant, and the inhibition rate of *FsveA*^{OEV14} on A549 cancer cells increased by about 14.69% (Fig. 3F, Table S4). Furthermore, it was also found by flow cytometry detection (Fig. S1, Table S5) that the apoptosis rate of the crude extract of the *FsveA* overexpression strain was significantly improve, about 4.86 fold than that of WT (Fig. 3G). This suggests that *FsveA* mediates the antitumor activity of *F. solani*.

FsveA mediates the production of antitumor substances in strains

To explore the substance basis of FsveA-mediated antitumor activity, the LC/MS non-targeted metabolomics method was used to detect metabolites of WT and *FsveA*^{OEV14} strains. Principal component analysis showed a significant separation between WT and *FsveA*^{OEV14} samples . Concomitantly, orthogonal partial least-squares discrimination analysis (OPLS-DA) also presented highly significant differences between the samples, all within 95% confidence intervals. And the results of hierarchical cluster analysis showed that the replicates of *FsveA*^{OEV14} and WT both formed separate branches, showing that there were indeed significant metabolic differences. The differential metabolites were further analyzed under the conditions of FC >1, P <0.05, and VIP >1, and it was found that 860 metabolites were co-expressed, of which 304 metabolites were up-regulated, 169 were down-regulated, and 387 metabolites had no difference (Fig. S3). *Via* Classification of detected differential metabolites based on the HMBD database, the main metabolites were carboxylic acids and derivatives, fatty acyl

groups, organic oxides, benzene and substituted derivatives, steroids and steroid derivatives (Fig. 4A). Also discovered were nucleosides (Zenchenko et al. 2021), terpenes (de Vasconcelos Cerqueira Braz et al. 2020), flavonoids (Pinto et al. 2021), phenols (Xia et al. 2021), indole derivatives (Han et al. 2020), and other compounds with potential antitumor activity. Furthermore, the metabolites were found to be significantly enriched in ABC transporter, purine metabolism, phenylalanine metabolism, 2-oxocarboxylic acid metabolism, aminoacyl- tRNA biosynthesis, and indole-like alkaloid metabolism *via* KEGG pathway enrich- ment analysis (Fig. 4B). It indicates that the regulation involved in *FsveA* is global and has a regulatory effect on the basal metabolism of the strain in addition to the regulation of secondary metabolism, which may be related to the mechanism of action of *FsveA*.

To excavate the differential metabolites associated with antitumor activity, KEGG enrichment network analysis was performed on the top 5 pathways of differential metabolites using the method of clusterProfiler selection hypergeometric test. The compounds in *FsveA*^{OEV14} that differed significantly from WT mainly belonged to alkaloids (pos_401 inosine, pos_5 adenosine, pos_117 riboflavin, pos_175 cytidine, and pos_471 carnitine), Carboxylic acid derivatives (pos_408 l-Arginine, pos_486 l-Methionine, etc), of which carnitine was 485 times more abundant than the WT(Fig. 4C). In addition to the compounds enriched in the above pathways, 24 candidate metabolites were screened with the conditions $\log_2$FC≥2, P <0.05, and VIP >1. Among the alkaloids, 2'-O-Methyluridine was only found in *FsveA*^{OEV14}, geldanamycin was up-regulated 3.98-fold compared with WT, Acadesine (AICAR) was up-regulated 5.31-fold compared to WT. The terpenes were all up-regulated, among which Geosmin was only found in *FsveA*^{OEV14}. In phenols 4-Allyl-2-methoxyphenol was up to 230.44- fold compared to WT. Cinnamaldehyde in aldehydes was up-regulated 52.9-fold compared to WT. Other carboxylic acid derivatives, flavonoids, fatty acyls, and unknown metabolites were also significantly up-regulated (Fig. 4D□Table S6). Taken together, it suggests that FsveA may mediate the production of multiple anti-tumor active substances in the strain.

FsveA mediates the expression of metabolic genes of antitumor active substances in the strain

To reveal the molecular basis of FsveA-mediated antitumor active substance, we analyzed the gene transcription patterns of WT and *FsveA*^{OE} using third-generation gene sequencing technology. The numerical control results showed that the data volume of both samples reached 6.26 GB, the sequencing depth met the analysis standard, the percentage of Q30 bases was above 94.91%, and the GC content of each sample was above 55.11% (Table S7). The above results indicated that the quality of transcriptome data was up to standard, and further analysis could be carried out. Differentially expressed genes (DEGs) were screened with $|\log_2$FC$|$ >1, P <0.05 as the criteria, and a total of 4536 differentially expressed genes were screened. In comparison with WT, the number of up-regulated differential genes in *FsveA*^{OEV14} was 1957, while the ones of down-regulated were 2579 (Fig. 5A). GO functional enrichment of differentially expressed genes then showed that 2964 genes in DEGs were clustered onto 59 functional categories (Fig. 5B). The largest number of genes was enriched in the metabolic process of biological processes with 1386 genes. Secondly, with 1163 genes in the cellular process, and the largest number of genes in the

membranes of cellular components, with 988 genes. About the molecular functions, the most abundant genes were involved in atalytic activity and molecular binding functions with 1342 and 1271 genes respectively. Combined with the classification of differentially expressed genes in KEGG, the highest number of DEGs involving the metabolic classes were found with 124 metabolic pathways including terpenoid biosynthesis, purine and pyrimidine metabolism, indole diterpene alkaloid biosynthesis, monolactam biosynthesis, 2-oxocarboxylic acid metabolism, ubiquinone and other terpenoid quinone biosynthesis, ABC transporters (Fig. 5C). These genes associated with metabolic pathways were all significantly different in *FsveA*^{OEV14} compared to those of WT, and the metabolic pathways of the enrichment were consistent with the metabolome enrichment results.

Based on the Pfam, Swissprot, and eggNOG class databases, we analyzed and summarized the metabolic differential genes enriched by GO and KEGG, and found that these differential genes belonged to 53 different families (Table S8). Among them, all 3-isopropylmalate dehydratases were up-regulated in *FsveA*^{OEV14}, and even the lowest expression was 5.30-fold higher than those in WT. And 43 DEGs in the fungal transcription factor Zn(2)-Cys(6) class were up-regulated with the highest up-regulation of 6.99-fold higher than those in WT. In the Glycosyl hydrolases family, 31 genes were up-regulated with the maximum up-regulation fold of 5.28 times. While 14 out of 15 Cytochrome P450 monooxygenases were significantly down-regulated compared to those in WT. Other pyridine nucleotide-disulfide oxidoreductases, FAD-dependent oxidoreductases, polyketide synthases, and ABC transporters were also up-or down-regulated significantly. To screen key genes associated with antitumor activity, 48 candidate key genes were screened *via* combining gene function annotations with $|\log_2 FC| > 1$, $P < 0.05$ and VIP >1 as the criteria (Fig. 6A, B; Table S9). Mainly including Glycosyl hydrolases family (Cheng et al. 2013; Yu et al. 2006), Zn(2)-Cys(6) class genes (Cai et al. 2020), Cytochrome P450 monooxygenases (Brandon et al. 2005), ABC transporter (Goossens et al. 2019; Shi et al.2022), 3-isopropylmalate dehyd -ratase (Wang, 2010), polyketide synthases (Bundale et al. 2018), Pyridoxal-phosp- hate-dependent enzyme (Li et al. 2020), α/β hydrolase class (Jaiswal et al. 2021) and Aminotransferase class (Luo et al. 2021), most of these candidate key genes have been reported in the literature to play an important role in the synthesis of antitumor substances and the mechanism of tumor activity. In addition, based on the information from the KEGG pathway annotation of each differential gene and each differential metabolite above, each differential gene and differential metabolite under the same KEGG pathway was correlated to understand the linkage between key genes and metabolites in the process of increased antitumor activity of *FsveA*^{OEV14}. The results showed that the differentially expressed metabolites and differentially expressed genes were significantly enriched in the combined pathways of pyrimidine metabolism, terpenoid backbone biosynthesis, ubiquinone and other terpenoid quinone biosynthesis, biotin metabolism, penicillin and cephalosporin biosynthesis and riboflavin metabolism (Fig. S4). This enrichment result was consistent with the KEGG results of metabolic analysis and transcriptional analysis. The above results jointly indicated that FsveA mediated the expression of the genes for the anti-tumor active substance metabolism in the strain.

To validate the reproducibility and repeatability of DEGs in transcriptome sequencing, five up-regulated and five down-regulated differential genes each were randomly selected from DEGs and validation analysis was performed by RT-qPCR (Fig. 6C, D; Table S2). The results were consistent with the transcriptome sequencing results, which confirmed that the transcriptome sequencing data were accurate (P <0.05).

Discussion

In this study, *via* overexpressing the global regulator *veA* in endophytic *Fusarium solani*, it was found that the antitumor activity of the crude extract of the overexpression mutant strain *viz FsveA*^{OEV14} was significantly improved in comparison with WT. The combined metabolomic and transcriptomic analyses has revealed that FsveA may mediate the expression of multiclass metabolic genes in the strain, thereby affecting antitumor substance biosynthesis.

According to metabolomics analysis, we found that multiple classes of substances were significantly different in *FsveA*^{OEV14} compared to WT, primarily comprising alkaloids, terpenes, carboxylic acid derivatives, phenols, aldehydes, and flavonoids. Most of these differential substances have promising potential for antitumor activity, and alkaloids account for a substantial proportion of antitumor drugs (Nussbaumer et al. 2011). In the differential substances we screened, the fraction of alkaloid compounds (including Geldanamycin, AICAR and Nucleosides) is likewise higher. Among them, Geldanamycin is reported to be a natural HSP90 inhibitor with good inhibitory activity against the growth of various tumor cells and has broad-spectrum anti-proliferative and anti-tumor effects (Xie et al. 2021). AICAR can induce apoptosis and inhibit migration and invasion of prostate cancer cells through the Ampk/Mtor-dependent pathway (Su et al. 2019). Adenosine is an important endogenous signaling molecule that can act as a ligand and participate in the regulation of various physiological and pathological processes such as apoptosis, cell proliferation, and vasodilation by binding to G protein-coupled receptors (Liu et al. 2020). Therefore, it is speculated that alkaloids play an important role in the antitumor activity of *FsveA*^{OEV14}. Terpenes are a broad class of compounds with a variety of promising physiological and pharmacological activities and are among the top anti-tumor agents currently being studied (de Vasconcelos Cerqueira Braz et al. 2020). Surprisingly, we also found that terpene substances (Lanosterin, Illudin M) were significantly enriched in *FsveA*^{OEV14} compared with WT. Lanosterin was reported to have a crucial role in the treatment of molecular diseases as well as cancer (Stäubert et al. 2016). Illudin M has anti-proliferative properties in various cancers, including prostate, kidney, pancreatic, breast, and lung cancers (Sharma et al. 2021). Thus, terpenes production may also contribute to the augmentation of the antitumor activity of *FsveA*^{OEV14}. In summarizing the differential substances, we found that although carboxylic acid derivatives (L-arginine), aldehydes (Cinnamaldehyde), phenols (4-Allyl-2-methoxyphenol) and flavonoids (Epicatechin gallate) accounted for a small ratio in comparison with alkaloids and terpenes, they were also significantly up regulated in *FsveA*^{OEV14}, and reported to have potential antitumor activity. Study has showed that L-arginine affects the metabolic fitness and viability of T cells which were critical for anti-tumor responses (Geiger et al. 2016). Cinnamaldehyde inhibits proliferation, migration,

invasion and promotes apoptosis of OS cells and is a potentially valid antitumor agent (Huang et al. 2020). 4-Allyl-2- methoxyphenol inhibits non-small cell lung cancer by inhibiting NF-B to regulate TRIM59 expression (Cui et al. 2019). Epicatechin gallate can be combined with other compounds to form novel agents that inhibit the tumorigenicity of human papillomavirus-positive head and neck squamous cell carcinomas (Piao et al. 2016). So it is implied that these classes of compounds also play an essential role in the antitumor activity of *FsveA*^{OEV14}. The above illustrates that FsveA mediates the production of multiple classes of substances, affecting the antitumor activity of *FsveA*^{OEV14}.

To shed light on the molecular basis of FsveA-mediated antitumor active substances, we screened 48 candidate key genes associated with the antitumor activity of *FsveA*^{OEV14} *via* transcriptome analysis, among which the most denotable ones are the glycosyl hydrolase family, Zn(2)-Cys(6)-like genes, cytochrome P450 monooxygenase, 3-isopropylmalate dehydratase, and polyketide synthases. The Glycosyl hydrolase family has an overriding role in catalyzing the glycosylation of substrates like oligosaccharides, fatty alcohols or aromatic alcohols, peptides, terpenes, phenolics, alkaloids and antibiotics (Cheng et al. 2013). It was discovered that this enzyme protein can efficiently catalyze the synthesis of paclitaxel precursors, which has promising applications in increasing the clinical availability of paclitaxel (Yu et al. 2006). In our metabolome analysis, it was speculated that the above class of enzymes may be intimately related to the production of a large number of alkaloids, terpenes, phenols, and other antitumor active substances in *FsveA*^{OEV14}. The Zn(2)-Cys(6) family of genes is a unique class of transcription factors found only in fungi and plays an essential regulatory role in basal metabolism, secondary metabolism, drug resistance, and meiosis in fungi (MacPherson et al. 2006). And it was discovered that this class of proteins can be used as tumor suppressors to inhibit hepatocellular carcinoma by inducing apoptosis of cell proliferation (Liang et al. 2017). *Via* transcriptome analysis, we found that these transcription factors were significantly up-regulated in *FsveA*^{OEV14} and were enriched in the biosynthesis of ubiquinone and terpenoid quinone. It implies that these classes of genes may regulate the production of terpenoid antitumor active substances in *FsveA*^{OEV14} or contribute directly to its antitumor activity. For the PKSs type of genes, it has long been documented that many newly discovered antibacterial, antitumor, and antiviral compounds are synthesized with these kinds of genes (Nikolouli et al. 2012). It has been demonstrated that the expression of these genes lead to improved production of the antitumor active substance *viz* geldanamycin [58] (Wang et al. 2017). Interestingly, our metabolomic analysis showed that the content of the alkaloid geldanamycin in *FsveA*^{OEV14} was also significantly larger compared to WT, further corroborating the close association of this class of genes with the production of antitumor active substances in *FsveA*^{OEV14}. The enzyme 3-isopropylmalate dehydratase participates in microbial amino acid synthesis and therefore exists in the vast majority of microorganisms (Wang, 2010). *Via* the KEGG enrichment of metabolome, transcript- ome, metabolome and transcriptome combined analyses, we unearthed that these enzymes were mainly involved in pyrimidine and purine metabolism. So it has being speculated that this class of enzymes may be mainly associated with alkaloidal antitumor active substances (Cytidine, Adenosine, Inosine) in *FsveA*^{OEV14}. Cytochrome P450 monooxygenase is a class of heme-containing oxidases encoded by a supergene

family that have long been shown to participate in the synthesis and metabolic reactions of terpenes, alkaloids, and sterols (Schuler et al. 2003). But some studies have illustrated that this class of enzymes has a promotive effect on tumor cell proliferation (Jiang et al. 2009). Surprisingly, *via* transcriptome analysis, we found that almost all of these enzymes were significantly down-regulated in *FsveA*^{OEV14} compared to WT. In the metabolome, the substances (including 20-HETE, 5-HETE, leukotrienes) corresponding to such genes was also significantly down-regulated in *FsveA*^{OEV14}compared with WT, or there was essentially no difference between the two. Hence we surmise that the high expression of *FsveA* caused the expression of this class of enzymes to be significantly down-regulated and the antitumor activity increased in *FsveA*^{OEV14}. In summary, FsveA overexpression may mediate the production of multiple classes of antitumor substances in *FsveA*^{OEV14}*via* multiple classes of genes direct or indirect regulation and result in the higher antitumor activity of *FsveA*^{OEV14} than WT-type strain.

Conclusion

Via overexpressing the global regulator *FsveA*, which conservely regulates in fungi, the antitumor activity of the crude extract from the overexpression mutant strain *viz FsveA*^{OEV14} was remarkably increased compared to WT. Multiple classes of antitumor active substances were screened by the metabolome, and 48 key genes that may be affiliated with antitumor activity were screened with combining database analysis of the transcriptome, revealing that the global regulator *FsveA* mediates the antitumor activity of endophytic *Fusarium solani*. Further studies may focus on validating, through biological experiments, how the anti-tumor activity attribute to these candidate genes or/and metabolites.

References

Akhberdi O, Zhang Q, Wang D et al (2018) Distinct Roles of Velvet Complex in the Development, Stress Tolerance, and Secondary Metabolism in *Pestalotiopsis microspora*, a Taxol Producer. Genes (Basel) 9: 164. ht tp://doi.org/10.3390/genes9030164

Alexander NJ, McCormick SP, Blackburn JA (2008) Effects of xanthotoxin treatment on trichothecene production in *Fusarium sporotrichioides*. Canadian Journal of Microbiology 54:1023-1031. http://doi.org/10.10 16/j.febslet.2007.08.062

Ameen F, Stephenson SL, AlNadhari S et al (2021) Isolation, identific- ation and bioactivity analysis of an endophytic fungus isolated from Aloe vera collected from Asir desert, Saudi Arabia. Bioprocess and biosystems engineering 44: 1063-1070. http://doi.org/10.1007/s0044 9-020-02507-1.

Assunção CB, de Aguiar EL, Al-Hatmi AMS et al (2020) New molec- ular marker for phylogenetic reconstruction of black yeast-like fungi (Chaetothyriales) with hypothetical EIF2AK2 kinase gene. Fungal Bi- ology 124: 1032-1038. http://doi.org/10.1016/j.funbio.2020.09.007.

Bedir E, Karakoyun Ç, Doğan G et al (2021) New Cardenolides from Biotransformation of Gitoxigenin by the Endophytic Fungus Alternaria eureka 1E1BL1: Characterization and Cytotoxic Activities. Molecules 26: 3030. http://doi.org/10.3390/molecules 26103030

Brandon EF, Meijerman I, Klijn JS et al (2005) In-vitro cytotoxicity of ET-743 (Trabectedin, Yondelis), a marine anti-cancer drug, in the Hep G2 cell line: influence of cytochrome P450 and phase II inhibition, and cytochrome P450 induction. Anticancer Drugs 16: 935-943. http: //doi.org/10.1097/01.cad.0000180121.16407.38

Bundale S, Singh J, Begde D et al (2018) Culturable rare actinomycetes from Indian forest soils: Molecular and physicochemical screening for biosynthetic genes. Iranian journal of microbiology 10: 132-142. http s://www.ncbi.nlm.nih.gov/pmc/articles/PMC6039449/

Cai J, Liu W, Wong CW et al (2020) Zinc-finger antiviral protein acts as a tumor suppressor in colorectal cancer. Oncogene pp: 5995-6008. ht tp://doi.org/10.1038/s41388-020-01416-7

Chen L, Zhang QY, Jia M et al (2016) Endophytic fungi with antitumor activities: Their occurrence and anticancer compounds. Critical reviews in microbiology 42: 454-473. https://doi.org/10.3109/1040841X.2014.959892

Cheng HL, Zhao RY, Chen TJ et al (2013) Cloning and characterization of the glycoside hydrolases that remove xylosyl groups from 7-β-xylosyl -10-deacetyltaxol and its analogues. Molecular and cellular proteomi- cs 12: 2236-2248. http://doi.org/10.1074/mcp.M113.030619

Chowdhury NS, Sohrab MH, Rana MS et al (2017) Cytotoxic Naphthoquinone and Azaanthraquinone Derivatives from an Endophytic *Fusarium solani*. Journal of Natural Products 80: 1173-1177. https://doi.org/10.1021/acs.jnatprod.6b00610

Cui Z, Liu Z, Zeng J et al (2019) Eugenol inhibits non-small cell lung cancer by repressing expression of NF-κB-regulated TRIM59. Phytoth -erapy research 33: 1562-1569. http://doi.org/10.1002/ptr.6352

de Vasconcelos Cerqueira Braz J, Carvalho Nascimento Júnior JA, Serafini MR (2020) Terpenes with Antitumor Activity: A Patent Review. Recent patents on anti-cancer drug discovery 15: 321-328. http://doi.org/10.2 174/1574892815666201002162315

Geiger R, Rieckmann JC, Wolf T et al (2016) L-Arginine Modulates T Cell Metabolism and Enhances Survival and Anti-tumor Activity. Cell. 167: 829-842. http://doi.org/10.1016/j.cell.2016.09.031

Geiser DM , Jiménez-Gasco MDM , Kang S et al (2004) FUSARIUM-ID v.1.0: A DNA sequence database for identifying *Fusarium*. European Journal of Plant Pathology 110: 473-479. http://doi.org/10.1023/B:EJ PP.0000032386.75915.a0

Goossens P, Rodriguez-Vita J, Etzerodt A et al (2019) Membrane Cholesterol Efflux Drives Tumor-Associated Macrophage Reprogra- mming and Tumor Progression. Cell metabolism 29: 1376-1389. http:

//doi.org/10.1016/j.cmet.2019.02.016

Han Y, Dong W, Guo Q et al (2020) The importance of indole and azaindole scaffold in the development of antitumor agents. European journal of medicinal chemistry 203: 112506. http://doi.org/10.1016/j.ejmech.20 20.112506

He Q, Zeng Q, Shao Y et al (2020) Anti-cervical cancer activity of secondary metabolites of endophytic fungi from Ginkgo biloba. Cancer Biomarkers 28: 371-379. http://doi.org/10.3233/CBM-190462

Huang YR, Chen J, Yang S et al (2020) Cinnamaldehyde Inhibits the Function of Osteosarcoma by Suppressing the Wnt/β-Catenin and PI3K/Akt Signaling Pathways. Drug design, development and therapy 14: 4625-4637. http://doi.org/10.2147/DDDT.S277160

Jaiswal S, Ayyannan SR (2021) Anticancer Potential of Small-Molecule Inhibitors of Fatty Acid Amide Hydrolase and Monoacylglycerol Lipase. ChemMedChem 16: 2172-2187. http://doi.org/10.1002/cmdc.202100120

Jiang JG, Shen GF, Chen C et al (2009) Effects of cytochrome P450 arachidonic acid epoxygenases on the proliferation of tumor cells. Chinese journal of cancer 28: 14-19. http://doi.org/10.1016/j.chb.2008.10.005

Katoh K, Standley DM (2013) MAFFT multiple sequence alignment software version 7: improvements in performance and usability. Molecular Biology and Evolution 30: 772-780. http://doi.org10.1093/molbev/mst010/

Kim HY, Han KH, Lee M et al (2009) The veA gene is necessary for the negative regulation of the veA expression in *Aspergillus nidulans*. Current genetics 55: 391-397. http://doi.org/10.1007/s00294-009-0253-y

Kopke K, Hoff B, Bloemendal S et al (2013) Members of the *Penicillium chrysogenum* velvet complex play functionally opposing roles in the regulation of penicillin biosynthesis and conidiation. Eukaryotic cell 12: 299-310. http://doi.org/10.1128/EC.00272-12

Li SJ, Zhang X, Wang XH et al (2018) Novel natural compounds from endophytic fungi with anticancer activity. European Journal of Medicinal Chemistry 156: 316-343. https://doi.org/10.1016/j.ejmech.2018.07.015

Li Z, Zhao Y, Zhou H et al (2020) Catalytic Roles of Coenzyme Pyridoxal-5'-phosphate (PLP) in PLP-dependent Enzymes: Reaction Pathway for Methionine-γ-lyase-catalyzed L-methionine Depletion. ACS catalysis 10: 2198-2210. http://doi.org/10.1021/acscatal.9b03907

Liang YH, Li Q, Chen K et al (2017) Zinc finger protein 307 functions as a tumor-suppressor and inhibits cell proliferation by inducing apoptosis in hepatocellular carcinoma. Oncology reports 38: 2229-2236. http:// doi.org/10.3892/or.2017.5868

Liu H, Kuang X, Zhang Y et al (2020) ADORA1 Inhibition Promotes Tumor Immune Evasion by Regulating the ATF3-PD-L1 Axis. Cancer Cell 37: 324-339. http://doi.org/10.1016/j.ccell.2020.02.006

Luo MY, Zhou Y, Liang Q et al (2021) Phosphoserine aminotransferase 1 mediates lung adenocarcinoma cell adhesion and its mechanism. Modern Biomedical Progress 21: 3601-3606. http://doi.org/10.13241/j.cnki.pmb.2021.19.001

Lyu HN, Liu HW, Keller NP et al (2020) Harnessing diverse transcriptional regulators for natural product discovery in fungi. Natural Product Report 37: 6-16. https://doi.org/10.1039/c8np00027a

Ma JC, Zhou Q, Zhou YH et al (2009) The size and ratio of homologous sequence to non-homologous sequence in gene disruption cassette influences the gene targeting efficiency in Beauveria bassiana. Applied Microbiology and Biotechnology 82: 891-898. http://doi.org/ 10.1007/s00253-008-1844-0

Ma Q, Liu YX, Liu ZY (2012) Research Progress of *veA* Gene in Filamentous Fungi. Guizhou Agricultural Sciences 40: 28-31. http://doi. org/CNKI:SUN:GATE.0.2012-03-010

MacPherson S, Larochelle M, Turcotte B (2006) A fungal family of transcriptional regulators: the zinc cluster proteins. Microbiology and Molecular Biology Reviews 70: 583-604. http://doi.org/10.1128/MMBR.00015-06

Nikolouli K, Mossialos D (2012) Bioactive compounds synthesized by non-ribosomal peptide synthetases and type-I polyketide synthases discovered through genome-mining and metagenomics. Biotechnology letters 34: 1393-1403. http://doi.org/10.1007/s10529-012-0919-2

Nussbaumer S, Bonnabry P, Veuthey JL et al (2011) Analysis of anticancer drugs: a review. Talanta 85: 2265-2289. http://doi.org/10.1016/j.talan ta.2011.08.034

Piao L, Mukherjee S, Chang Q et al (2016) TriCurin, a novel formulation of curcumin, epicatechin gallate, and resveratrol, inhibits the tumorigenicity of human papillomavirus-positive head and neck squamous cell carcinoma. Oncotarget 8: 60025-60035. http://doi.org/ 10.18632/oncotarget.10620

Pinto C, Cidade H, Pinto M et al (2021) Chiral Flavonoids as Antitumor Agents. Pharmaceuticals (Basel, Switzerland) 14: 1267. http://doi.or g/10.3390/ph14121267

Qiu F , Xu G , Xie CP et al (2020) Identification of *Fusarium solani* causing basal stem and root rot of Crossandra infundibuliformis in Hainan, China. Australasian Plant Pathology 49: 605-608. http://doi.org/10. 1007/s13313-020-00735-3

Ran XQ, Zhang G, Li S et al (2017) Characterization and antitumor activity of camptothecin from endophytic fungus *Fusarium solani* isolated from Camptotheca acuminate. African health sciences 17: 566-574. https://doi.org/10. 4314/ahs.v17i2.34

Schuler MA, Werck-Reichhart D (2003) Functional genomics of P450s. Annual Review of Plant Biology 54: 629-667. http://doi.org/10.1146/ annurev.arplant.54.031902.134840

Shan HC, Ma WG, Gao ZZ (2005) Research progress of natural antitumor drugs in China. Journal of Modern Traditional Chinese and Western Medicine 14: 825 -827. https://doi.org/10.3969/j.issn.1008-8849.2005.06.127

Sharma B, Kumar V (2021) Has Ferrocene Really Delivered Its Role in Accentuating the Bioactivity of Organic Scaffolds? . Journal of medicinal chemistry 64: 16865-16921. http://doi.org/10.1021/acs.jmedchem.1c00390

Shi R, Zhao K, Wang T et al (2022) 5-aza-2'-deoxycytidine potentiates anti-tumor immunity in colorectal peritoneal metastasis by modulating ABC A9-mediated cholesterol accumulation in macrophages. Therano- stics 12: 875-890. http://doi.org/10.7150/thno.66420

Soni SK, Singh R, Ngpoore NK et al (2021) Isolation and characteri- zation of endophytic fungi having plant growth promotion traits that biosynthesizes bacosides and withanolides under in vitro conditions. Brazilian journal of microbiology 52: 1791-1805. http://doi.org/10.10 07/s42770-021-00586-0

Stäubert C, Krakowsky R, Bhuiyan H et al (2016) Increased lanosterol turnover: a metabolic burden for daunorubicin-resistant leukemia cells. Medical oncology 33: 6. http://doi.org/10.1007/s12032-015-0717-5

Su CC, Hsieh KL, Liu PL et al (2019) AICAR Induces Apoptosis and Inhibits Migration and Invasion in Prostate Cancer Cells Through an AMPK/mTOR-Dependent Pathway. International journal of molecular sciences 20: 1647. http://doi.org/10.3390/ijms20071647

Teixeira TR, Santos GSD, Armstrong L et al (2019) Antitumor Potential of Seaweed Derived-Endophytic Fungi. Antibiotics (Basel) 8: 205. https://doi.org/10.3390/ antibiotics8040205

Terkar A, Borde M (2021) Endophytic fungi: Novel source of bioactive fungal metabolites. New and Future Developments in Microbial Biotechnology and Bioengineering pp: 95-105. https://doi.org/10.1016/B978-0-12-821005-5.00006-5

Ur Rashid H, Rasool S, Ali Y et al (2020) Anti-cancer potential of sophoridine and its derivatives: Recent progress and future perspectives. Bioorganic Chemistry 99: 103863. https://doi.org/10.1016/j.bioorg.2020.103863

Vaidya G, Lohman DJ, Meier R (2011) SequenceMatrix: concatenation software for the fast assembly of multi-gene datasets with character set and codon information.Cladistics-the International Journal of the Willi Hennig Society 27: 171-180. http://doi.org/10.1111/j.1096-0031. 2010.00329.x

Wang C (2010) Study on the enzymatic properties of Cytophaga hutchinsonii α-isopropylmalate synthase. Shandong University. http:// doi.org/10.7666/d.y1790917

Wang XR, Ning X, Zhao Q et al (2017) Improved PKS Gene Expression With Strong Endogenous Promoter Resulted in Geldanamycin Yield Increase. Biotechnology journal 12. http://doi.org/10.1002/biot.201700321

Wei Q, Bai J, Yan D et al (2021) Genome mining combined metabolic shunting and OSMAC strategy of an endophytic fungus leads to the production of diverse natural products. Acta Pharm Sin B 11: 572-587. https://doi.org/10.1016/j.apsb.2 020.07.020

White T, Bruns T, Lee S et al (1990) Amplification and direct sequencing of fungal ribosomal RNA genes for phylogenetics. PCR protocols: a guide to methods and applications pp: 315-322. http://doi.org/10.0000/PMID1793

Xia TT, Li J, Ren X et al (2021) Research progress of phenolic compounds regulating IL-6 to exert antitumor effects. Phytotherapy research 35: 6720-6734. http://doi.org/10.1002/ptr.7258

Xie J, Liu J, Liu H et al (2015) The antitumor effect of tanshinone IIA on anti-proliferation and decreasing VEGF/VEGFR2 expression on the human non-small cell lung cancer A549 cell line. Acta Pharm Sin B 5: 554-563. http://doi.org/10.1016/j.apsb.2015.07.008

Xie YH, Guo L, Huang J et al (2021) Cyclopentenone-Containing Tetrahydroquinoline and Geldanamycin Alkaloids from Streptomyces malaysiensis as Potential Anti-Androgens against Prostate Cancer Cells. Journal of natural products 84: 2004-2011. http://doi.org/10.10 21/acs.jnatprod.1c00297

Xu K, Gao Y, Li YL et al (2018) Cytotoxic p-Terphenyls from the Endolichenic Fungus Floricola striata. Journal of natural products 81: 2041-2049. http://doi.org/10.1021/acs.jnatprod.8b00362

Yu HL, Xu JH, Lin GQ (2006) Overview of glycoside hydrolases in glycoside synthesis. Organic Chemistry 26: 1052-1058. http://doi.or g/10.3321/j.issn:0253-2786.2006.08.004

Zenchenko AA, Drenichev MS, Il'icheva IA et al (2021) Antiviral and Antimicrobial Nucleoside Derivatives: Structural Features and Mechanisms of Action. Molecular biology 55: 786-812. http://doi.org/10.1134/S0026893321040105

Zhang FA, Liu SR , Zhou XJ et al (2020) *Fusarium xiangyunensis* (Nectriaceae), a remarkable new species of nematophagous fungi from Yunnan, China. Phytotaxa 450: 273-284. http://doi.org/10.11646/phytotaxa.450.3.3

Zhu X, Li H, Long L et al (2012) miR-126 enhances the sensitivity of non-small cell lung cancer cells to anticancer agents by targeting vascular endothelial growth factor A. Acta biochimica et biophysica Sinica 44: 519-526. http://doi.org/10.1093/abbs/gms026

Declarations

Funding This work was supported by National Natural Science Foundation of China under Grant (No. 32170019、32160667、31901947).

Conflicts of interest/Competing interests The authors declare no conflict of interest.

Author contributions Jichuan Kang, Zhangjiang He conceived and designed the experiments. Lu Cai performed the experiments, analyzed the data, contributed to manuscript preparation and editing, and wrote the paper. Jiankang Wang and Yongjie Li contributed to the construction of the genetic transformation system. Min Qin and Xueming Yin prepared material for cell experiments. All authors have read and approved the manuscript.

Availability of data and materials All material and data are stored at Guizhou University, College of Pharmacy, Guiyang, People's Republic of China, and may be shared upon request directed to the corresponding author.

Ethics approval Compliance with ethical standards. Human alveolar adenocarcinoma cell (A549) cells were purchased from Xiamen Immocell Biotechnology Co., Ltd.

Consent for publication No individual data are presented in this manuscript.

Figures

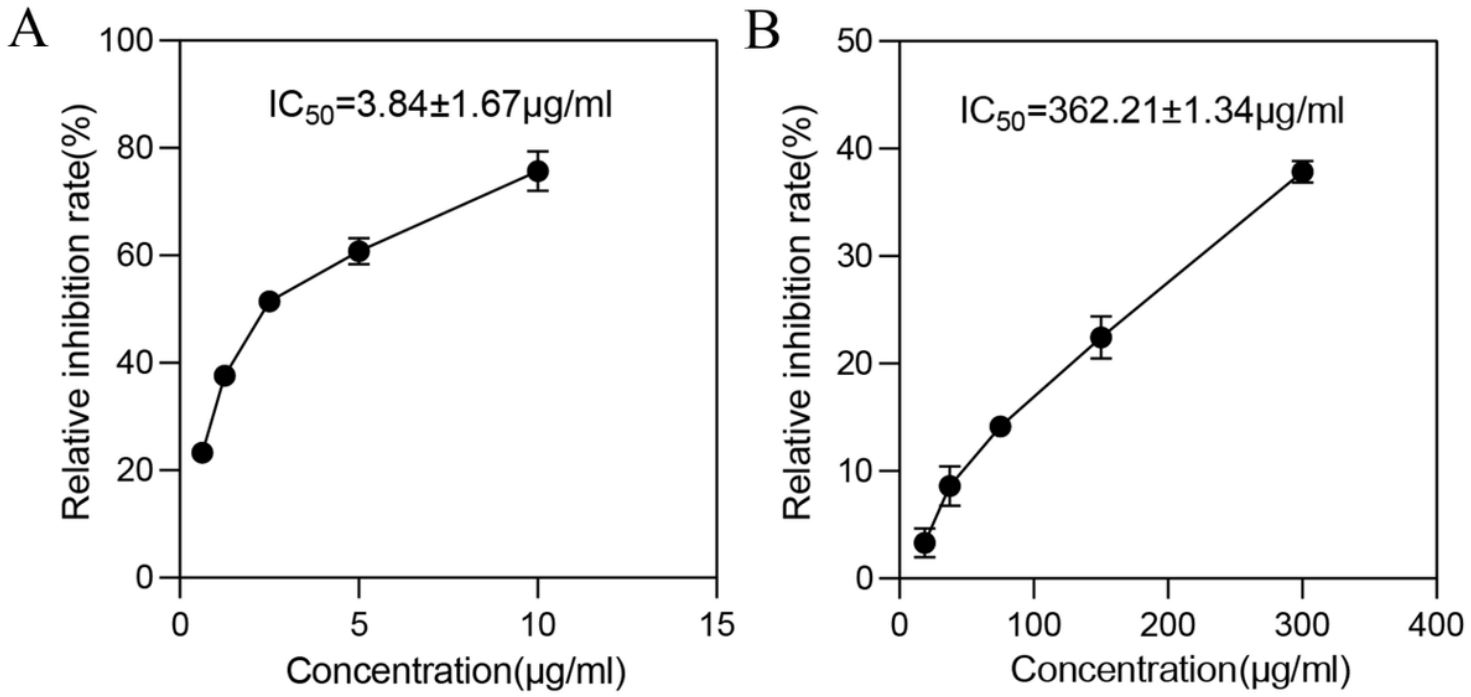

Figure 1

The crude extracts of endophytic Fusarium solani have anti-tumor activity. A, Relative inhibition rates of adriamycin at different concentrations on A549 cancer cells; B, Relative inhibition rate of different

concentrations of crude extract of HB1-J1 on A549 cancer cells; the experiment was repeated three times, and the mean values were taken, the error bars were standard deviations (±SD)

Figure 2

Fusarium solani morphology and phylogenetic tree. A, Colony morphology on PDA medium; B-D, Different types of conidiogenous structures; E-F, Chlamydospore; G, Large and small conidia; H, Phylogenetic tree constructed with multi-gene tandem of ITS , EF1α, RPB1 and RPB2 sequences; scale bars□c-g=10 μm

Figure 3

Inhibition of A549 growth by crude extracts of WT and *FsveA*^{OEV14} strains. A, Comparative diagram of FsveA homologous protein; B, Schematic diagram of *FsveA*^{OE} mutant vector construction; C, The WT strain and randomly selected transformants were grown on a CZM plate containing hygromycin B (20 μg/mL) resistance; D, PCR validation of transformants using the hygromycin B resitance gene carried by the pK_2*hyg*-PgpdA-veA vector, M: Star marker D2000, Positive control: pK_2*hyg*-PgpdA-veA plasmid; E, Analysis of relative expression of *FsveA* gene in WT and *FsveA*^{OE} strains; F, Relative Inhibition Rate of WT and *FsveA*^{OEV14} Extracts on A549 Cells by MTT; G, Apoptosis of A549 cells induced by WT and *FsveA*^{OEV14} extracts was detected by the AnnexinV-FITC/PI assay; the experiment was repeated three times and the mean values were taken, error bars are standard deviations (±SD), **P* <0.05, ***P* <0.01, ****P* <0.005, *****P* <0.001

Figure 4

Global analysis of the metabolic profiles of WT and *FsveA*^{OEV14} strains. A, HMDB differential metabolite classification chart, which shows only the top 20 metabolic classifications in descending order; B, Enrichment chart of differential metabolite pathways, where the horizontal axis is the number of differential metabolites annotated to the pathway and the vertical axis is the pathway name; C, KEGG enrichment network diagram of differential metabolites, the light yellow nodes in the diagram are pathways, the small nodes connected to them are specific metabolites annotated to the pathway, the diagram shows up to 5 pathways; D, Enrichment diagram of 24 key differential metabolites, the hierarchical clustering of differential metabolites in WT and *FsveA*^{OEV14} shows two different branches, comparing the significant characteristics of specific metabolism of *FsveA*^{OEV14} to those of WT, the clustering display diagram done with the average expression of differential metabolites in WT and *FsveA*^{OEV14}

Figure 5

Analysis of DEGs. A, Volcano plot of differentially expressed genes. Each point in the plot represents a gene. The horizontal coordinate indicates the logarithmic value of the expression ploidy difference of a gene in two samples, the larger its absolute value, the greater the expression ploidy difference between the two samples. The vertical coordinate indicates the negative logarithmic value of the false discovery rate, the larger its value, the more significant the differential expression and the more reliable the differentially expressed genes obtained by screening. In the plot green and red dots represent genes with significant expression differences, green represents down-regulated gene expression, red represents up-regulated gene expression, and black dots represent genes with no significant expression differences; B, GO secondary node annotation statistics of differentially expressed genes, where the vertical coordinate is the GO classification, the top horizontal coordinate is the percentage of the number of genes, and the bottom horizontal coordinate is the number of genes; C, KEGG classification of differentially expressed genes, where the vertical coordinate is the name of the KEGG metabolic pathway, the horizontal coordinate is the number of genes annotated to the pathway, and the percentage of the total number of genes annotated

Figure 6

Expression of critical genes. A-B, Clustered heat maps of up- and down-regulated key gene expressions obtained from the screening, where each column represents a sample, different rows represent different genes, and the colors represent the logarithmic values of the gene expression FPKM in the sample with a base of 2; C-D, QRT-PCR verification of transcriptome data, among them, c28192. graph_c0: 3-isopropylmalate dehydratase, c27832. graph_c1: Zn(2)-Cys(6)SUC1, c31126. graph_c1: Protein SnodProt1, c32983. graph_c0: PRELI/MSF1 protein, c37044. graph_c0: Ribose-phosphate pyrophosphkinase were selected from the up-regulated DEGs for verification; among the down-regulated DEGs, c37592. graph_c0: Glycerol-3-phosphate dehydrogenase, c35536. graph_c1: Enoyl-(Acyl carrier protein) reductase, c38759. graph_c0: Glycosyl hydrolases, c20458. graph_c0: Epoxide hydrolase srdG, c15521. graph_c0: Cytochrome P450 monooxygenase FCK2 were selected for verification, the experiment was repeated three times, and the mean was taken. Error bars are standard deviation (±SD), $*P < 0.05$, $***P < 0.005$

Supplementary Files

This is a list of supplementary files associated with this preprint. Click to download.

- attachmenttomanuscript.rar